Proceedings of the ASME 2023
International Design Engineering Technical Conferences and
Computers and Information in Engineering Conference
IDETC/CIE2023
August 20–23, 2023, Boston, MA

DETC2023-XXXXXX

KIRIGAMI CORRUGATIONS: STRONG, MODULAR, AND PROGRAMMABLE PLATE LATTICES

Alfonso Parra Rubio[1,†,*], Klara Mundilova[2,†,*], David Preiss[1], Erik D. Demaine[2], Neil Gershenfeld[1]

[1]Center for Bits and Atoms, Massachusetts Institute of Technology, Cambridge, MA
[2]Computer Science and Artificial Intelligence Laboratory, Massachusetts Institute of Technology, Cambridge, MA

ABSTRACT

Plate lattices are high-performance lightweight structures, exhibiting up to twice the yield strength and stiffness compared to truss lattices of similar geometric arrangement and relative density. Although they are of great interest for research and structural engineering applications, their complex manufacturing and assembly processes limit their practical use, with sandwich panels being an exception. This paper presents a novel approach to the design and modular assembly of folded custom 3-dimensional plate lattices as structural corrugations for use in structural engineering and robotics applications. The plate lattice structural corrugation uses a building block strategy and incorporates custom modified unit cells based on the Miura-ori. This transformation involves expanding the top and bottom zig-zag crease lines into facets and orienting them in space. The resulting modified pattern is referred to as the Kirigami Expanded Miura. The unique structure of these lattices not only provides exceptional mechanical performance as static structures, but also allows for the design of anisotropies in their flexural stiffness by alternating between the Maxwell criterion on bending-dominated or stretch-dominated cells. These anisotropies can have value differences of up to 24 with the same geometry, making them ideal for robotic morphing applications. We validate our proposed technology by characterizing the mechanical performance of this new building system and comparing it with state-of-the-art corrugations. We demonstrate the potential of this approach by designing, manufacturing, and modularly assembling multiple structures and robots with single and double curvature.

Keywords: Kirigami, origami, robotics, doubly curved structures

1. INTRODUCTION

Architected materials are ubiquitous and extensively used across diverse industries, including aerospace, architecture, furniture, and packaging. These materials possess a distinctive characteristic, whereby their properties, whether mechanical, thermal, or acoustic, are predominantly dictated by their geometrical arrangement, rather than their material composition.

From the perspective of lightweight engineering, architected materials enabled the creation of structures with superior mechanical performance at low mass cost. This has significantly benefited industries such as aerospace, automotive, naval, and wind power, enabling them to construct structures that push the limits of what can be achieved at the same mass budget.

Sandwich structures are widely utilized architected materials, irrespective of their core structure. The transition from monocoque to sandwich panel fuselages in the de Havilland Mosquito [1] marked the beginning of industrialized production of sandwich panels, particularly those with honeycomb cores. These panels offer superior flexural rigidity per unit mass and unit cost compared to monolithic materials [2]. However, Honeycombs encounter issues with moisture absorption within their cells during operation [3], high costs for small production runs, inefficient milling processes for creating 3-dimensional shapes [2], and anticlastic deformations when bent to form curved panels [1].

Numerous studies have proposed new core geometries to address these issues. Open-cell geometries [4] made from metals [5] and composites [6] were first proposed as alternative truss-based cores. However, they encounter challenges in providing accurate 3D shapes and suffer from labor-intensive manufacturing methods. Another proposal is flexible cells for monoclastic deformation, which are intended for use in morphing structures [7] [8]. Nevertheless, these cells have an encapsulated volume that absorbs moisture and encounter difficulties in providing custom 3D shapes.

Folding approaches play a big role in core structure research. Kirigami-inspired methods allow for the creation of complex single curvature [9], doubly curvature [2], and custom stiffness [10] while also encapsulating closed volumes. Other folded strategies have been proposed to tackle shape, moisture ingress and high

[†]Joint first authors
[*]Corresponding author: aprubio@mit.edu, kmundil@mit.edu

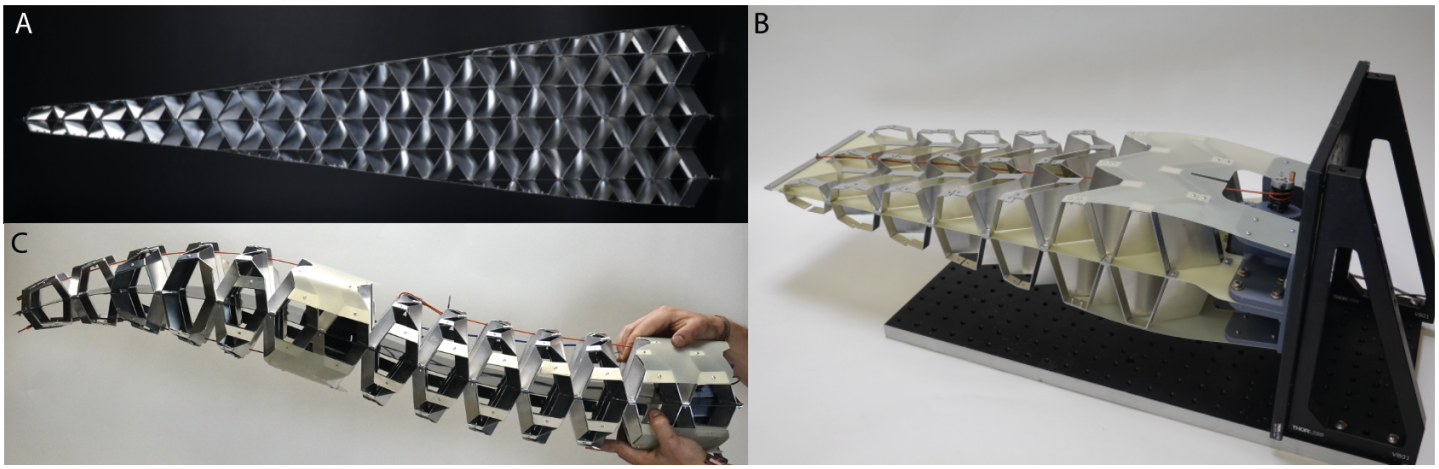

FIGURE 1: A) HTP CROSS SECTION OF PASSENGER AIRCRAFT BUILD WITH KIRIGAMI CORRUGATIONS. B) MORPHING WING. C) DOUBLY CURVED ARGE SCALE TENTACLE WITH TWO DOF.

structural efficiency using Miura-ori folds [11] [12] [13], but it is still a challenge to generate custom doubly curved shapes.

Additionally, all of the aforementioned core geometries share two significant inflexibilities. First, they are primarily designed for static applications. Second, the interface between the core material and the sandwich surface is at points or edges, necessitating the use of structural adhesives, welding or co-curing strategies for assembly.

Our work introduces a novel family of structural corrugations for static and dynamic engineering applications. Our Kirigami based approach provides solutions to the aforementioned issues and extends the traditional use of sandwich structures, overcoming their inherent limitations.

We show the potential of Kirigami based solutions by first introducing the *Kirigami Expanded Miura*, which is a modification of the well-known Miura-ori crease pattern. This transformation removes the dependency of using structural adhesives, by faceting contact between the new core and the top and bottom surfaces. This allows for more accessible, reversible, and recyclable joining methods such as bolting and riveting. Additionally, the open cell nature of this core eliminates issues related to water ingress.

Second, we demonstrate how custom folded cores can be generated without the need for post-processing operations to adapt the core material to a 3D target surface.

Third, we show how this geometry can expand the classic use of sandwich structures by introducing the concept of corrugations with controlled flexural stiffness, by selecting which cells satisfy the Maxwell Stability Criterion. This approach opens up new design possibilities for morphing structures and robotics using structural corrugations.

Fourth, we introduce the idea of discrete origami, a method for simplifying assembly of crease patterns by splitting a pattern into simple unit cells. This opens the door to assemble larger scale structures.

Finally, we validate our approach through experimental testing and practical applications, including the creation of multiple static structures and robots.

2. METHODS

Our studied structural corrugation is a variation of the well-known Miura-ori pattern, which is a rigidly and flat foldable origami pattern consisting of parallelograms (see Figure 2). The Miura-ori pattern has two families of creases:

- One family of creases lies on parallel zig-zag polylines. Their mountain or valley assignment is constant along a single polyline, but alternates between neighboring zig-zag polylines. We will refer to those creases in their folded state as *xy-corrugations*.
- The other family of creases lies on y-parallel lines. On a single line, the crease assignments alternate between mountain and valley folds. We will refer to those creases in their folded state as *yz-corrugations*.

Miura-ori patterns have applications as foldcores [14], where the folded pattern is sandwiched between two planes that contain the folded zig-zag creases. However, joining the Miura-ori pattern along the folded zig-zag creases with the the sandwich planes is challenging. To simplify the mechanical joining between the corrugation and the adjacent structure (such as a centroid for continuum robotics, a skin for a facade, or other corrugation to assemble cellular materials), we conduct experiments with a modification of the Miura-ori crease pattern (see Fig. 2). This modification transforms the vertices of the tessellation into facets to enable a wider range of joining methods for structural use, e.g., bolting, riveting, co-curing, or gluing. The new faces are added by extruding the creases of the tessellation to faces. To preserve developability of the pattern, we remove some of the extruded faces (namely the added non-rectangular faces), resulting in a *Kirigami Expanded Miura* tessellation.

In the following section, we first show the modification of the Miura-ori pattern. We then discuss how we customize the pattern to fill the space between a planar and a curved boundary. The resulting *customized Kirigami Expanded Miura* pattern needs additional cuts to be developable. Finally, we provide some fabrication-specific modification details.

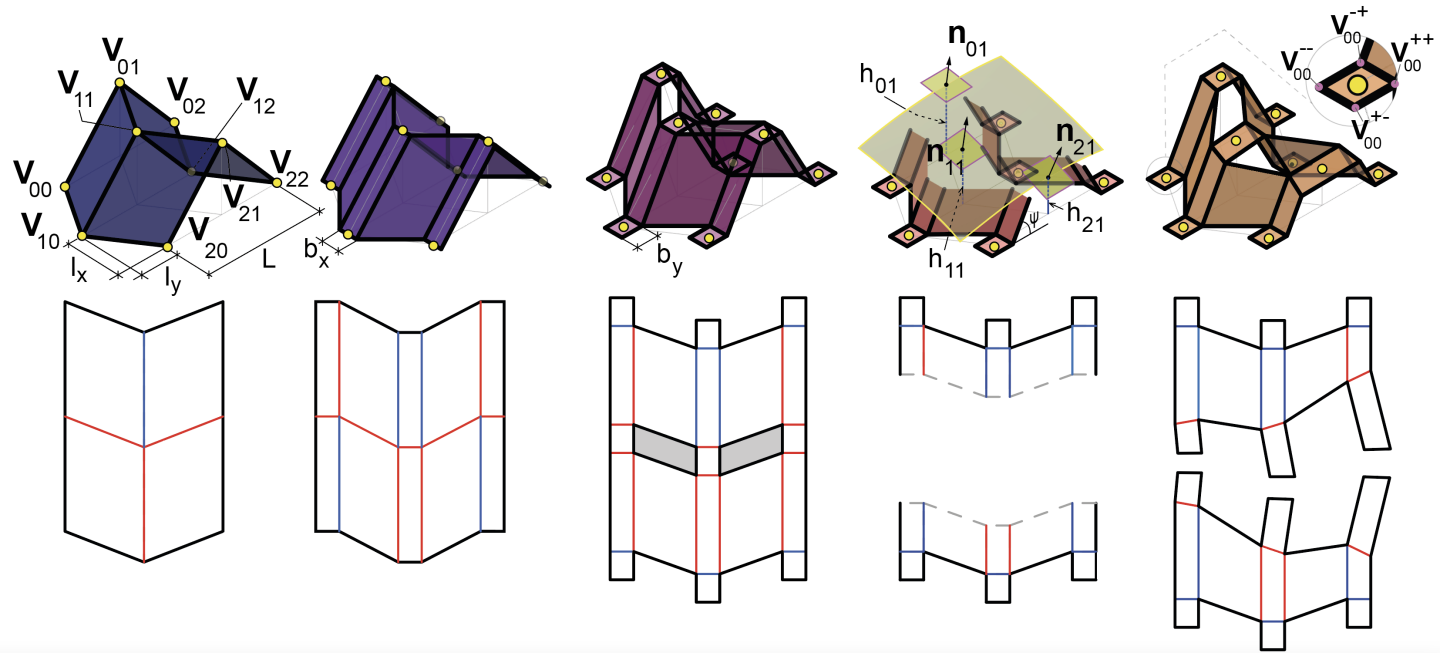

FIGURE 2: TRANSFORMATION FROM MIURA-ORI TO KIRIGAMI EXPANDED MIURA.

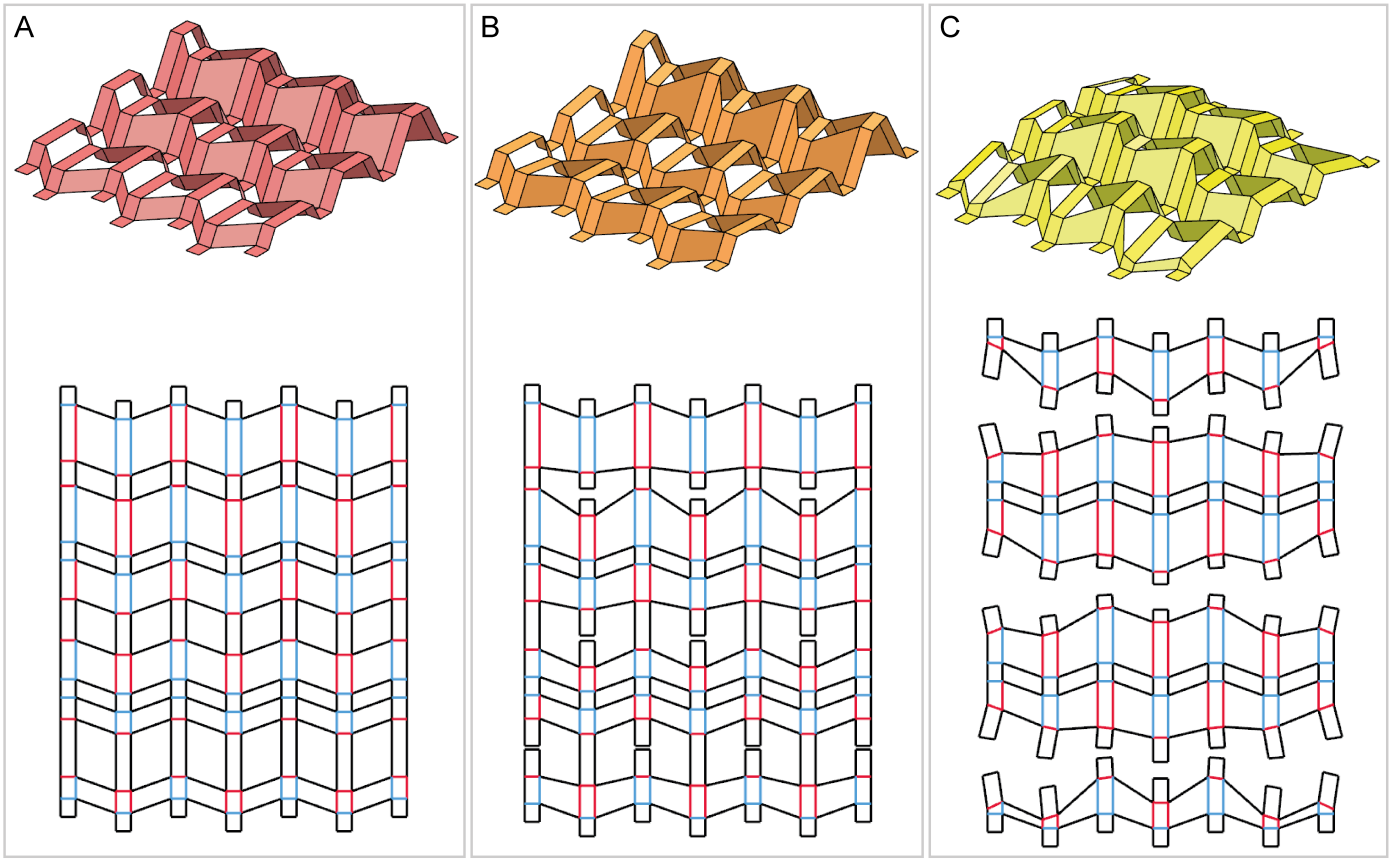

FIGURE 3: A) *xy*-PARALLEL PLANES, NO CUTS NEEDED. B) SINGLE CURVATURE. C) DOUBLY CURVATURE.

2.1 Miura-Ori

The studied pattern modification starts with a folded state M of a the Miura-ori pattern sandwiched between two xy-parallel planes Π_1 and Π_2. It is known that the vertex locations $\mathbf{V}_{i,j}$ of a folded state of a $(n_x \times n_y)$-Miura-ori pattern can be uniquely constructed from four parameters [15]; see Figure 2:

- two parameters $l_x > 0$ and $l_y > 0$ that specify the zig-zag shape of the xy-corrugation,
- a distance L between two neighbouring xy-corrugations with same crease assignment,
- a distance h between the two sandwich planes Π_1 and Π_2.

For $0 \le i < n_x$ and $0 \le j < n_y$, the vertices of the folded state can then be written as

$$\mathbf{V}_{i,j} = \left(l_x i, \frac{L}{2} j + r_{i+1} l_y, r_j h \right), \tag{1}$$

where r_k is the remainder of k when dividing by two.

2.2 Kirigami Expanded Miura

Similar to [11], the considered modification of the Miura-ori pattern first extrudes the yz-corrugations by $\frac{b_x}{2}$ in x-parallel direction to both sides. This splits each vertex $\mathbf{V}_{i,j}$ of M into two vertices $\mathbf{V}^+_{i,j}$ and $\mathbf{V}^-_{i,j}$, that is,

$$\mathbf{V}_{i,j} \;\mapsto\; \mathbf{V}^{\pm}_{i,j} = \mathbf{V}_{i,j} \pm \left(\frac{b_x}{2}, 0, 0 \right) \quad \text{where} \quad 0 < b_x < l_x. \tag{2}$$

The resulting modified tessellation M' has new rectangular faces corresponding to the yz-corrugations of M, and new creases of length b_x in the zig-zag polylines, resulting in *modified xy-corrugations*. Note that M' is still rigidly foldable, but not flat foldable as the sum of opposite angles of a vertex does not add up to π.

Second, we extrude the modified xy-corrugations of M' by $\frac{b_y}{2}$ in y-parallel direction to both sides. This splits each vertex $\mathbf{V}^{\pm}_{i,j}$ of M' into two vertices $\mathbf{V}^{\pm+}_{i,j}$ and $\mathbf{V}^{\pm-}_{i,j}$, that is,

$$\begin{aligned} \mathbf{V}^{+}_{i,j} &\;\mapsto\; \mathbf{V}^{+\pm}_{i,j} = \mathbf{V}^{+}_{i,j} \pm \left(0, \tfrac{b_y}{2}, 0 \right), \\ \mathbf{V}^{-}_{i,j} &\;\mapsto\; \mathbf{V}^{-\pm}_{i,j} = \mathbf{V}^{-}_{i,j} \pm \left(0, \tfrac{b_y}{2}, 0 \right), \end{aligned} \quad \text{where} \quad 0 < b_y < l_y. \tag{3}$$

The resulting modified tessellation M'' has two types of new faces, rectangles and parallelogram. The former correspond to extruded vertices of M, the latter to the extruded zig-zag creases of M', respectively. This modification breaks the developability of the pattern, as the sum of angles around a vertex does not equal 2π. We therefore remove the newly added parallelogram faces (areas colored in grey in Fig. 2) to obtain the Kirigami Expanded Miura pattern M''.

The pattern M'' contains three types of faces. We call the faces that lie in the lower sandwich plane Π_1 *bottom faces*, the faces that lie in the upper sandwich plane Π_2 the *top faces*, and all other faces *inclined*. Note that the vertices of the initial Miura pattern M coincide with the centers of the top and bottom faces of M''.

2.3 Customized Kirigami Expanded Miura

In the following, we discuss how to customize the Kirigami Expanded Miura pattern to fill the area between the xy-plane Π_{xy} and a smooth, well-behaved surface Σ corresponding to a 3D function by appropriate "trimming". In general, this results in a corrugation that requires additional cuts for developability, see Section 2.4. However, we found that separation into unit-cells or strips is beneficial for fabrication.

2.3.1 User-Input. Imitating Section 2.1, we assume that the user specifies the intended supporting points $\mathbf{V}_{i,j}$ of the corrugation by three lengths (l_x, l_y, L). In addition, instead of a single height h, we assume that we are given reasonable target heights $h_{i,j}$ and reasonable target normal vectors $\mathbf{n}_{i,j}$ of the top faces (that is, for odd j) of the corrugation. Furthermore, the user can specify the dimensions (b_x, b_y) of the lower base planes, and the inclination angle ψ of the rectangular faces corresponding to the extruded yz-corrugation (see Figure 2).

2.3.2 Construction. The provided user-input allows us to define the *base points* of the corrugation by modifying Equation (1) to

$$\mathbf{V}_{i,j} = \left(l_x i, \frac{L}{2} j + r_{i+1} l_y, r_j h_{i,j} \right).$$

For each bottom base point, we construct the bottom faces $\{\mathbf{V}^{++}_{i,j}, \mathbf{V}^{-+}_{i,j}, \mathbf{V}^{+-}_{i,j}, \mathbf{V}^{--}_{i,j}\}$ as in Equations (2) and (3).

For odd j, let $\Pi_{i,j}$ be the *top base plane* incident to $\mathbf{V}_{i,j}$ that is orthogonal to $\mathbf{n}_{ij}$. To obtain the vertices of the modified top faces, we define $\mathbf{v}_{\pm} = (0, \pm\cos\psi, \sin\psi)$ and intersect the top base planes with $\mathbf{v}_{\pm}$-parallel lines containing the corners of adjacent lower faces, resulting in

$$\begin{aligned} \mathbf{V}^{--}_{i,j} &= \mathbf{V}^{-+}_{i-1,j} + \frac{\left(\mathbf{V}^{-+}_{i-1,j} - \mathbf{V}_{i,j} \right) \cdot \mathbf{n}_{ij}}{\mathbf{v}_{+} \cdot \mathbf{n}_{ij}} \mathbf{v}_{+}, \\ \mathbf{V}^{+-}_{i,j} &= \mathbf{V}^{++}_{i-1,j} + \frac{\left(\mathbf{V}^{++}_{i-1,j} - \mathbf{V}_{i,j} \right) \cdot \mathbf{n}_{ij}}{\mathbf{v}_{+} \cdot \mathbf{n}_{ij}} \mathbf{v}_{+}, \\ \mathbf{V}^{-+}_{i,j} &= \mathbf{V}^{--}_{i+1,j} + \frac{\left(\mathbf{V}^{--}_{i+1,j} - \mathbf{V}_{i,j} \right) \cdot \mathbf{n}_{ij}}{\mathbf{v}_{-} \cdot \mathbf{n}_{ij}} \mathbf{v}_{-}, \\ \mathbf{V}^{++}_{i,j} &= \mathbf{V}^{+-}_{i+1,j} + \frac{\left(\mathbf{V}^{+-}_{i+1,j} - \mathbf{V}_{i,j} \right) \cdot \mathbf{n}_{ij}}{\mathbf{v}_{-} \cdot \mathbf{n}_{ij}} \mathbf{v}_{-}, \end{aligned}$$

the corners of the constructed top faces. Let the union of the corners of the top and lower faces be the vertices of the customized Kirigami Extruded Miura such that is has the same face topology as the corresponding Kirigami Extruded Miura.

2.4 Development

Note that in most cases, the customized Kirigami Extruded Miura is not developable without additional cuts that result in connected components of groups of faces. In this section, we discuss how to obtain a crease pattern with at most $\lceil \frac{n_y}{2} \rceil$ connected components. Note however, that often times it might be beneficial

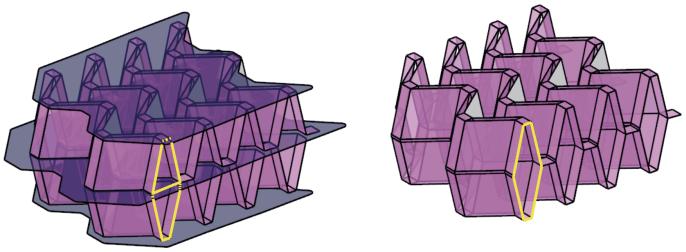

FIGURE 4: LEFT) STRETCH DOMINATED CELL. RIGHT) BENDING-DOMINATED CELL. BOTH HIGHLIGHTED IN YELLOW.

to define even smaller groups of connected faces, as discussed in Section 2.7.

First, observe that the inclined creases of the customized Kirigami Extruded Miura are parallel. We thus can join the adjacent inclined faces into a single developable strip. Furthermore, as the bottom base planes are rectangles, and the bottom holes are congruent, we can join two strips of inclined faces by the developed bottom faces.

In the case that the Kirigami Extruded Miura is cut with xy-parallel planes, the top faces are also congruent. Therefore, we can join two strips of inclined faces by the developed top faces. This results in a global development without additional cuts.

If however, the top surface is constant in x-direction (the normals are orthogonal to the x-axis, and the heights alternate between points on the same zig-zag), the top faces are still rectangles, but of different size. Furthermore, the dimensions of the top faces alternate between points on the same zig-zag. By making a cut in every second top face, we can again join two strips of inclined faces by every second top face.

Finally, for doubly curved surfaces, the top faces are in general not rectangular. We can thus only unroll pairs of strips of inclined faces joined along the bottom faces and attached top faces, resulting in $\lceil \frac{n_y}{2} \rceil$ groups of faces.

2.5 Custom compliance

One of the objectives of this paper is to provide corrugated structures that can be used dynamically in robotics or morphing structures.

In cellular solid theory, the Maxwell Stability Criterion determines whether the lattice microstructure deformation is bending-dominated or stretch-dominated. Studies have shown that, at the same relative density values, stretch-dominated geometries have significantly higher stiffness and strength than bending-dominated geometries [16]as shown in Fig.4 . Here we show how this geometrical characteristic can be utilized to selectively lower the flexural modulus in specific sections of our corrugation, enabling us to actuate these sections using tendon actuation.

2.6 Actuation

Actuation was achieved by tensioning steel wire tendons routed across the surface of locally compliant regions of the structure, as shown in Figure 8. Actuator modules consisted of closed-loop brushed DC motors, each with a 160:1 gear reduction, and a PID position controller running at 5 kHz. Custom dual-shaft pulleys were used to simultaneously spool and unspool a pair of tendons on opposite sides of the centroid, to allow for bending in either direction, without overconstraining the structure.

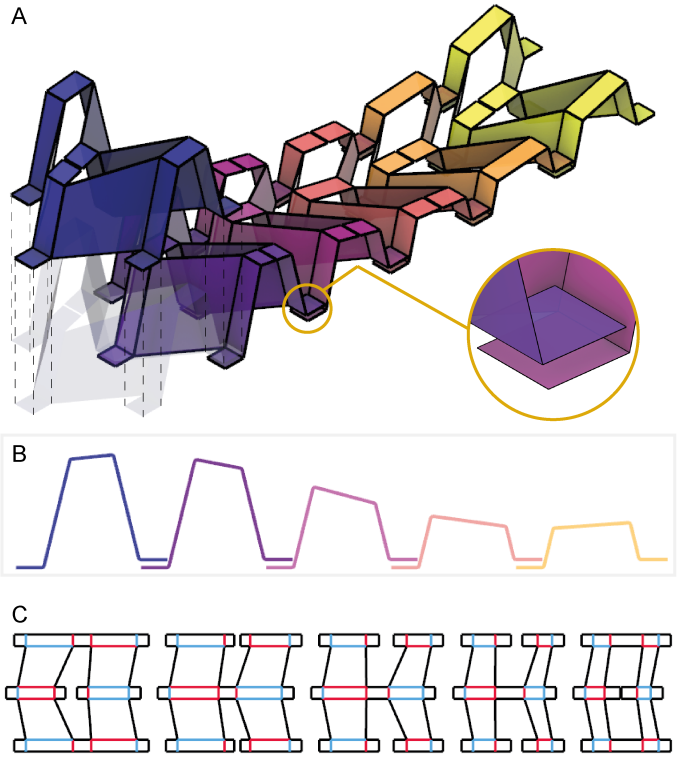

FIGURE 5: DISCRETELY ASSEMBLED ORIGAMI. A) STRUCTURAL SHAPED CORE. THE FIRST CELL SHOWS ITS ASSEMBLY MOTION. ZOOM DETAIL OF THE CELL TO CELL JOIN. B) SCHEME OF THE DISCRETELY ASSEMBLED CORRUGATION. C) CREASE MAP OF THE CELLS IN A.

2.7 Modular assembly: Discrete Origami

Most folding patterns exhibit kinematics similar to a parallel mechanism, where the crease pattern responsible of the formation of a desired 3D shape follows a continuous rigid-folding motion. This motion entails a change in the angle of planar neighbor facets composing the creases [17]. However, the challenge of finding a manufacturing method that meets the geometric constraint of only bending the creases without in-plane stressing of the stock material facets is highly intricate.

To address this kinematic issue, we propose a modularly constructed origami, as illustrated in Fig. 5. This approach involves isolating the unit cell that constitutes the tessellation and discretely assembling each cell to its adjacent cell using the same boundary conditions. Our proposal offers two key advantages: First, it reduce the overall number of creases, simplifying the manufacturing process. Simpler crease patterns can be accomplished through well-known methods such as cold metal forming, double face milling, or perforated creases. Second, it enables the construction of arbitrarily large structures, as the discrete nature of the process removes the manufacturing method size constraint from the overall size of the structure [18].

2.8 Fabrication-specific Implementation Details

The above mentioned decomposition has the drawback that additional joining is needed. Our fabricated models have overlaps between adjacent unit-cells and strips, which results in some of the base faces becoming doubly-covered. To ease fabrication, we incorporate material thickness in our implementation. In particular, we offset the overlapping faces and trim by a small amount (see Fig. 5). If the joint is made by riveting, we carefully place holes into pairs of top and bottom faces.

2.9 Manufacturing and Assembly

We fabricate our specimens using the router module RM-A of a Zund G-3 L-2500 equipped with a 2mm end mill R502. The material used is Hylite, a 1.2mm aluminum composite panel from 3A Composites that consists of a 0.8mm polypropylene core sandwiched between two layers of 0.2mm aluminum.

Taking advantage of the stacked configuration of the material we double face mill the crease pattern. Firstly, when designing the crease pattern, we add registration marks and decompose it into two parts, isolating peaks and valleys. We mirror one of the isolated crease patterns along the axis that we will later flip our material on. Then, using the machine, we first mill the registration marks and engrave the first creases to a depth of 0.6mm. Next, we flip the stock material along the aforementioned axis and using the registration module of the Zund, we locate the previously milled reference points and proceed to mill the rest of the creases with the same depth values. In this step we also mill the holes needed to assemble the structure using rivets. This results in distributing peaks to one side of the aluminum composite and valleys to the opposite side, enabling clean folding of the material with minimal bending strain.

3. RESULTS

Here we evaluate the compressive and flexural behavior of folded corrugations through experimental testing. Eight specimens underwent axial-load compression and three-point bending testing using an Instron 5985 with a 250 kN load cell. Both experiments were conducted at a rate of $10\frac{mm}{min}$. Data acquisition was performed using the Bluehill 3 software. In the case of the 3-point bending test, the support diameters were designed according to ASTM D790 standards. All specimens shared the same unit cell, with the following parameters: $L = 68mm$, $b_x = b_y = 11mm$, $\psi = 70^o$, $l_x = 28.5mm$, $l_y = 29.5mm$, and thickness = $1.2mm$.

3.1 Compression loading

We performed uniaxial compression test to four specimens with different architectures:

- **s1**: is a continuum origami specimen of 2 by 2 by 3 cells.
- **s2**: is a discrete origami specimen of 2 by 2 by 3 cells with stretch-dominated cells.
- **s3**: is a discrete origami specimen of 2 by 2 by 3 cells with bending dominated cells.
- **s4**: is a straight corrugation for comparison.

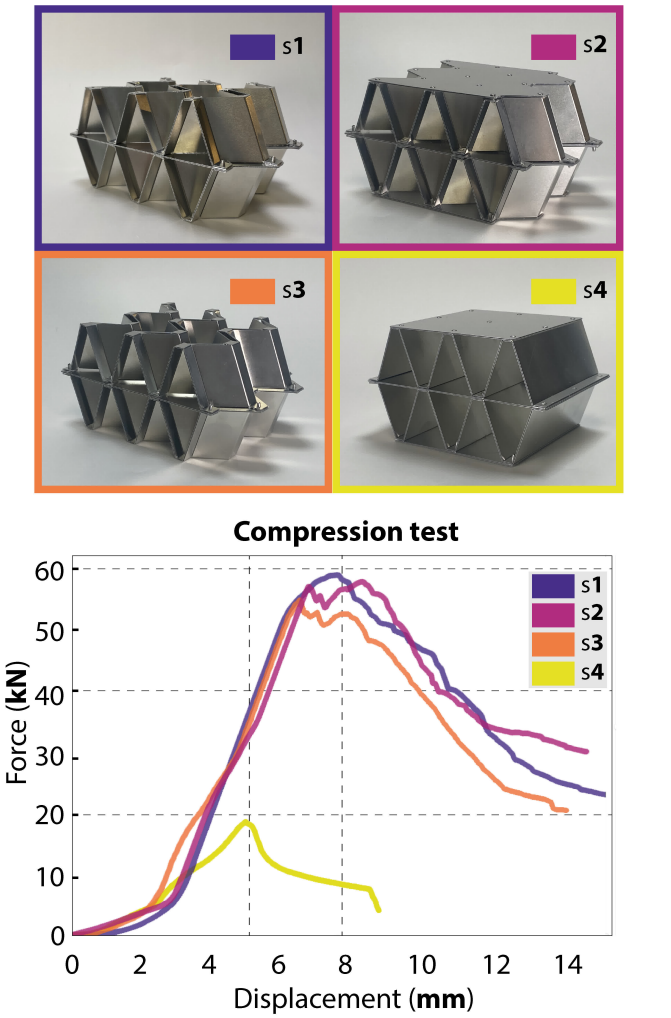

FIGURE 6: TOP) SPECIMENS WITH CORRESPONDING LABELS. BOTTOM) FORCE-DISPLACEMENT PLOT OF ALL SPECIMENS TESTED.

The performance of the four specimens can be seen in Table 1 and Fig. 6.

Our findings, presented in Table 1 and Fig. 6, demonstrate that there is no distinction in behavior between continuum and discrete origami assemblies.

Furthermore, stretch-dominated and bending-dominated unit cells exhibited similar behavior during uniaxial compression.All Kirigami Extended Miura geometries were found to withstand up to three times the maximum load of a conventional corrugation with the same geometry and relative density value. Additionally, the breaking mode of the Kirigami Extended Miura demonstrated a much more ductile behavior, with the ability to absorb more energy when collapsing compared to the straight corrugation.

3.2 Bending flexural loading

In the interest of simplicity of assembly, and after validating no mechanical performance differences between continuum and discrete corrugations for our current sample size, we have opted to use discrete origami for all samples in this study.

We quantified the anisotropy of flexural modulus for a

TABLE 1: UNIAXIAL COMPRESSION TEST RESULTS

	$S1$	$S2$	$S3$	$S4$
Specimen width (mm)	132	132	132	132
Specimen height (mm)	100	102.4	100	102.4
Specimen length (mm)	212	212	212	184
Effective Density ($\frac{kg}{m^3}$)	91.1	110.6	91.3	112.3
Effective Strength (MPa)	2.1	2.07	1.9	0.67
Effective Elastic Modulus (MPa)	64.7	50	47.5	37.7
Load:mass ratio	24000:1	19000:1	21000:1	7000:1

TABLE 2: THREE-POINT BENDING TEST RESULTS

	$S5$	$S6$	$S7$	$S8$
Specimen width (mm)	152	132	132	152
Specimen height (mm)	102.4	102.4	102.4	102.4
Specimen length (mm)	483	492	492	483
Effective Density ($\frac{kg}{m^3}$)	102.6	131	112.2	94.4
Bending Stiffness (EI, $N.m^2$)	184	136	9.23	8.63
Normal Force:Displacement ratio ($\frac{N}{mm}$)	221:1	158.5:1	11:1	10.6:1

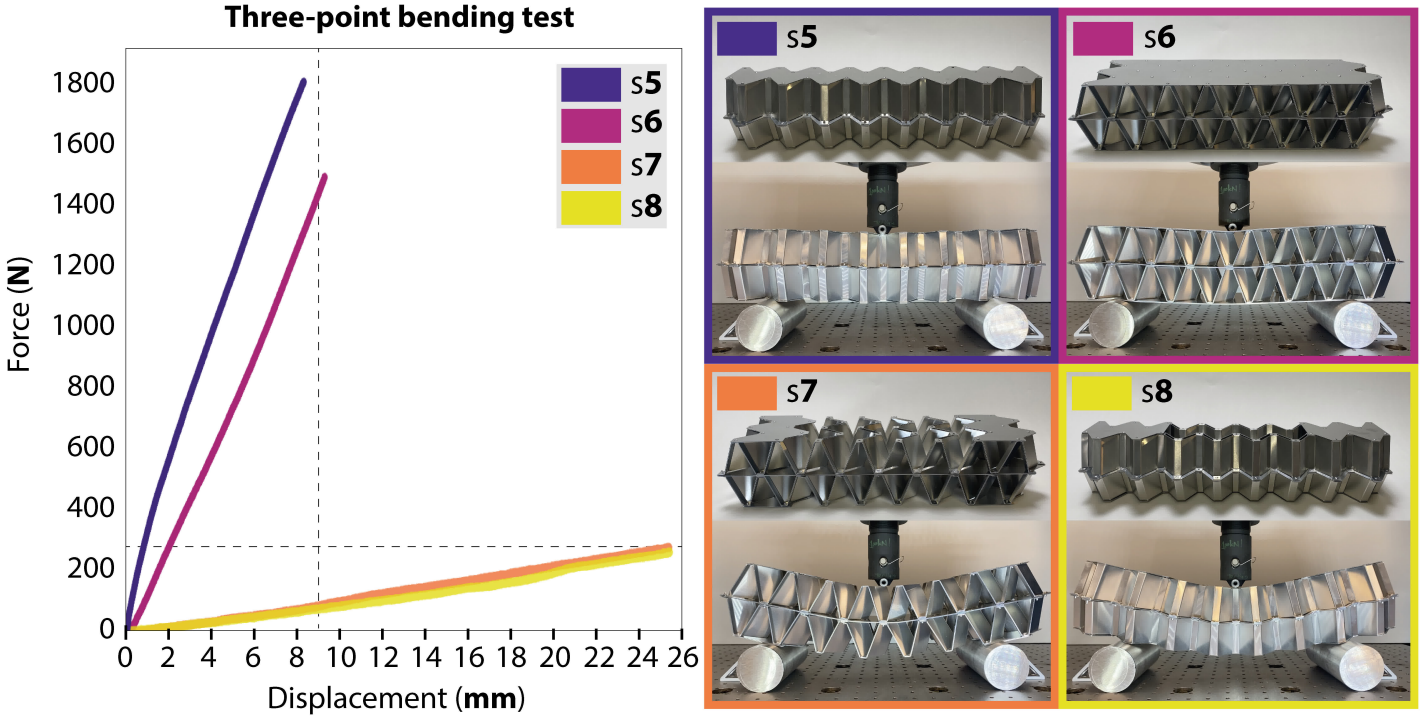

FIGURE 7: LEFT) FORCE-DISPLACEMENT OF THE FOUR SAMPLES UNDER A THREE-POINT BENDING TEST. RIGHT) CORRESPONDING SAMPLES WITH MAXIMUM DEFLECTION IMAGES

given geometry by comparing stretch-dominated and bending-dominated cells. To accomplish this, we conducted three-point bending tests on four specimens with different architectures:

- **s5**: 8 by 2 by 2 beam of cells oriented towards the y-axis in a stretch-dominated architecture.
- **s6**: 8 by 2 by 2 beam of cells oriented towards the x-axis in a stretch-dominated architecture.
- **s7**: 8 by 2 by 2 beam of cells oriented towards the y-axis in a bending-dominated architecture.
- **s8**: by 2 by 2 beam of cells oriented towards the x-axis in a

bending-dominated architecture.

Figure 7 and Table 2 summarize experimental results. Comparing S5 with S8 and S6 with S7, we observed a significant difference in flexural rigidity values between architectures dominated by stretching and those dominated by bending, ranging from 14 to 21.3 times. Furthermore, both architectures exhibited similar flexural rigidity values in orthogonal axes, indicating isotropic behavior of the corrugation in the two principal axes.

3.3 Static structures and robots manufacturing

We constructed multiple structures and robots using Kirigami corrugations. Figure 8 depicts two robots presented in this paper: a single degree of freedom, single curvature morphing wing and a large-scale, two degree of freedom, doubly curved tentacle. Figure 9 displays static structures with single and double curvature.

4. CONCLUSION

Our work focuses on designing custom shaped high-performance structural corrugations using folding approaches. This geometry not only exhibit significant compressive load capacity but also provides the ability to selectively behave stiff or compliant in bending loads.

These lightweight structures have an immediate application for medium - large scale robotic applications. Besides, they hold potential in the aerospace sector for new morphing-load bearing structures. Furthermore, the discrete manufacturing method simplifies the assembly of large models and enables the scalability of these structures to architectural scales. In our future work, we plan to explore the energy absorption capabilities of these plate-based structures, with potential applications in the automotive industry.

To demonstrate the potential, we modified the Miura-ori into the Kirigami expanded Miura pattern and developed equations for folding and unfolding it to fit arbitrary surfaces. We introduced the concept of discrete origami to simplify folded structures into smaller crease patterns that can be assembled modularly. We conducted mechanical testing and validated our approach by building static structures and robots.

ACKNOWLEDGMENTS

This work was supported by the Center for Bits and Atoms Research Consortia. Klara Mundilova is supported by the AAUW International Fellowship and the GWI Fay Weber Grant.

REFERENCES

[1] Zenkert, Dan. *An Introduction to Sandwich Structures* (1995). DOI 10.1115/MSEC2018-6646.

[2] Calisch, Sam and Gershenfeld, Neil. "Towards Continuous Production of Shaped Honeycombs.": p. V003T02A007. 2018. DOI 10.1115/MSEC2018-6646.

[3] Cise, Lakes R.S., D. "Moisture ingression in honeycomb core sandwich panel." 1997. DOI https://doi.org/10.1007/s11665-997-0074-4.

[4] Wicks, Nicole and Hutchinson, John. "Optimal Truss Plates." *International Journal of Solids and Structures - INT J SOLIDS STRUCT* Vol. 38 (2001). DOI 10.1016/S0020-7683(00)00315-2.

[5] Wadley, H.N.G., Fleck, Norman and Evans, Anthony. "Fabrication and Structural Performance of Periodic Cellular Metal Sandwich Structures." *Composites Science and Technology* Vol. 63 (2003): pp. 2331–2343. DOI 10.1016/S0266-3538(03)00266-5.

[6] Finnegan, K., Kooistra, G., Wadley, H.N.G. and Deshpande, V.S. "The compressive response of carbon fiber composite pyramidal truss sandwich cores." *International Journal of Materials Research - INT J MATER RES* Vol. 98 (2007): pp. 1264–1272. DOI 10.3139/146.101594.

[7] Chen, Yijin, Scarpa, Fabrizio, Remillat, Chrystel, Farrow, Ian, Liu, Yanju and Leng, Jinsong. "Curved Kirigami SILICOMB cellular structures with zero Poisson's ratio for large deformations and morphing." *Journal of Intelligent Material Systems and Structures* Vol. 25 No. 6 (2014): pp. 731–743. DOI 10.1177/1045389X13502852. URL https://doi.org/10.1177/1045389X13502852, URL https://doi.org/10.1177/1045389X13502852.

[8] Ozdemir, Nazli, Scarpa, Fabrizio, Craciun, Monica, Remillat, Chrystel, Lira, Cristian, Jagessur, Yogesh and Rocha-Schmidt, Luiz. "Morphing nacelle inlet lip with pneumatic actuators and a flexible nano composite sandwich panel." *Smart Materials and Structures* Vol. 24 (2015). DOI 10.1088/0964-1726/24/12/125018.

[9] Saito, Kazuya, Pellegrino, Sergio and Nojima, Taketoshi. "Manufacture of Arbitrary Cross-Section Composite Honeycomb Cores Based on Origami Techniques." Vol. 136. 2013. DOI 10.1115/DETC2013-12743.

[10] Calisch, Sam. "Folded Functional Foams." 2019. MIT. URL https://cba.mit.edu/docs/theses/19.09.calisch.pdf.

[11] Hähnel, Falk, Wolf, Klaus, Hauffe, Andreas, Alekseev, Kirill and Zakirov, Il'dus. "Wedge-shaped folded sandwich cores for aircraft applications: From design and manufacturing process to experimental structure validation." *CEAS Aeronautical Journal* Vol. 2 (2011). DOI 10.1007/s13272-011-0014-8.

[12] Miura, Koryo. "Zeta-Core Sandwich-Its Concept and Realization." *ISAS report/Institute of Space and Aeronautical Science,University of Tokyo* Vol. 37 No. 6 (1972): pp. 137–164. URL https://cir.nii.ac.jp/crid/1050848249892668672.

[13] Neville, Robin and Scarpa, Fabrizio. "Design of Shape Morphing Cellular Structures and Their Actuation Methods." 2015. DOI 10.13140/RG.2.1.4530.1527.

[14] Miura, Koryo. *Zeta-Core Sandwich- Its Concept and Realization*. Institute of Space and Aeronautical Science, University of Tokyo (1972).

[15] Schenk, Mark and Guest, Simon D. "Geometry of Miura-folded metamaterials." *Proceedings of the National Academy of Sciences* Vol. 110 No. 9 (2013): pp. 3276–3281. DOI 10.1073/pnas.1217998110. URL https://www.pnas.org/doi/abs/10.1073/pnas.1217998110.

[16] Gibson, Lorna J. and Ashby, Michael F. "Cel-

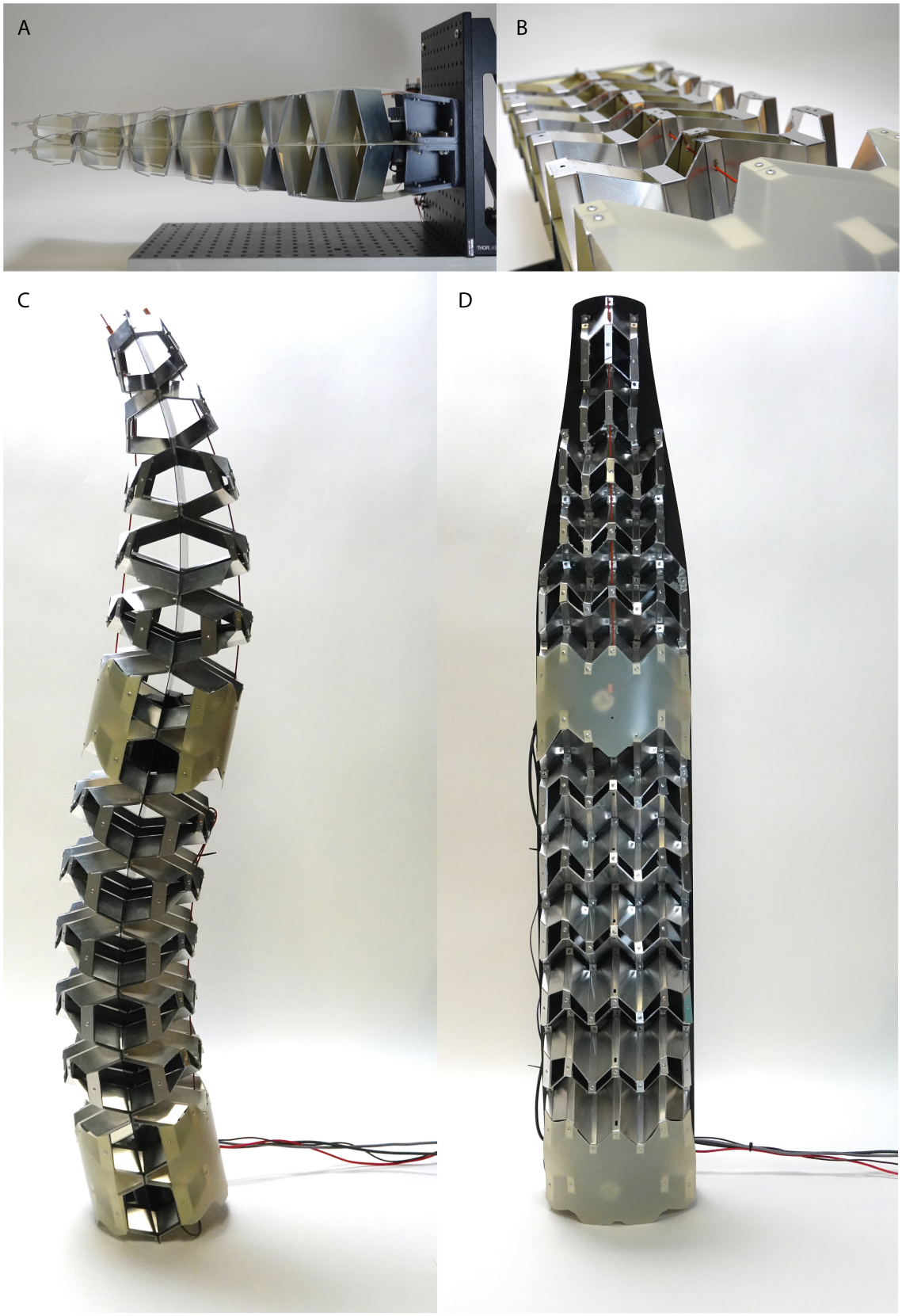

FIGURE 8: A) SIDE VIEW OF THE ACTUATED MORPHING WING. B) DETAILED IMAGE OF THE TENDON ROUTING SYSTEM. C AND D) SIDE AND FRONT VIEW OF THE LARGE SCALE 2 DOF TENTACLE.

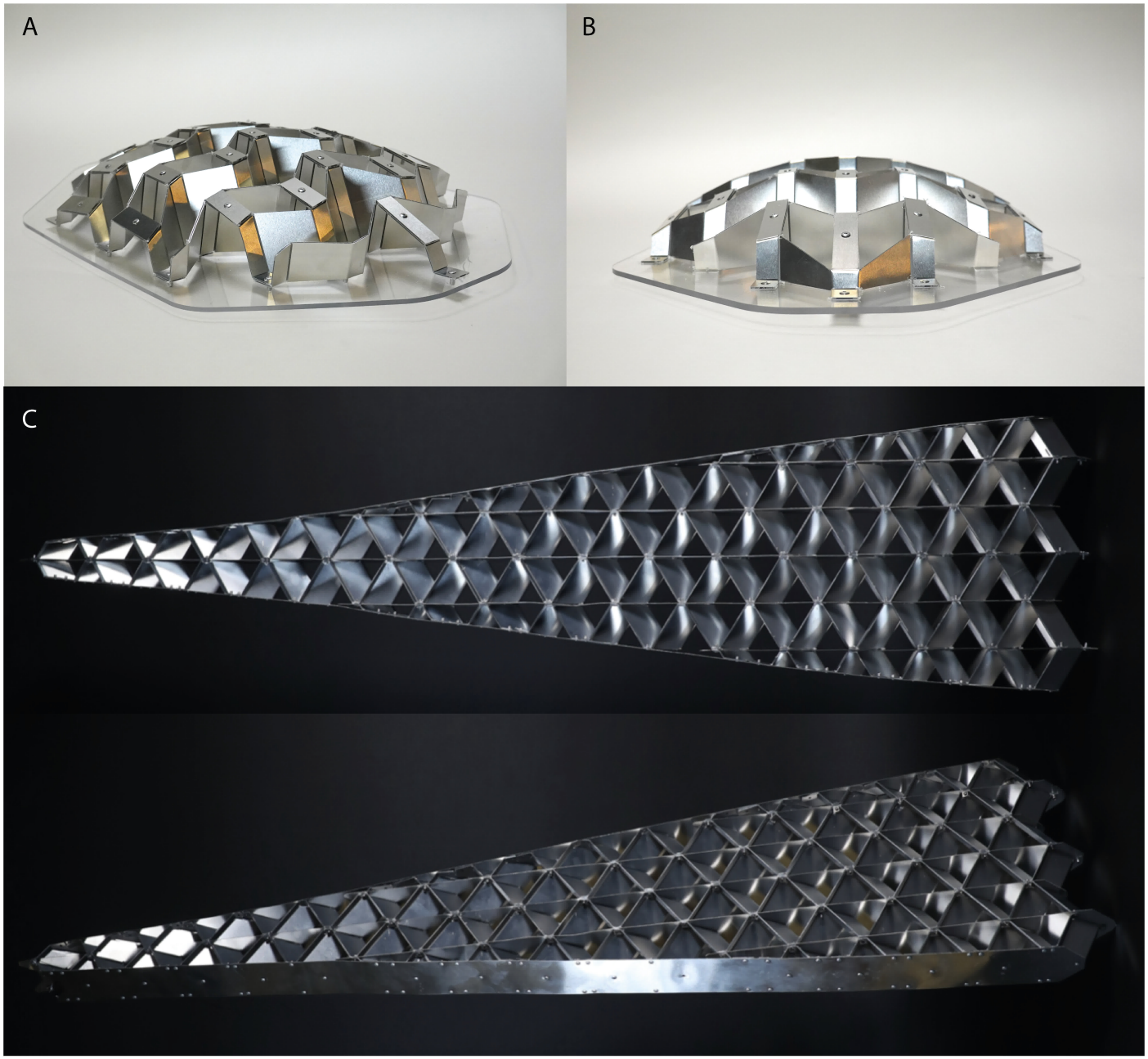

FIGURE 9: A AND B) DOUBLY CURVED SHELL. C) 1:1 SCALE OF THE CROSS SECTION OF AN HTP OF A SINGLE AISLE TRANSATLANTIC AIRPLANE.

lular Solids: Structure and Properties." (1997)DOI 10.1017/CBO9781139878326.

[17] Akitaya, Hugo, Demaine, Erik D., Horiyama, Takashi, Hull, Thomas C., Ku, Jason S. and Tachi, Tomohiro. "Rigid Foldability is NP-Hard." (2018)DOI 10.48550/ARXIV.1812.01160. URL https://arxiv.org/abs/1812.01160.

[18] Jenett, Benjamin, Cameron, Christopher, Tourlomousis, Filippos, Rubio, Alfonso Parra, Ochalek, Megan and Gershenfeld, Neil. "Discretely assembled mechanical metamaterials." *Science Advances* Vol. 6 No. 47 (2020): p. eabc9943. DOI 10.1126/sciadv.abc9943. URL https://www.science.org/doi/pdf/10.1126/sciadv.abc9943, URL https://www.science.org/doi/abs/10.1126/sciadv.abc9943.